Geometrically Interlocking Space-Filling Tiling Based on Fabric Weaves

Vinayak R. Krishnamurthy, Ergun Akleman, Sai Ganesh Subramanian, Matthew Ebert, Jiaqi Cui, Chia-an Fu, Courtney Starrett

Abstract—In this paper, we introduce a framework for the geometric design and fabrication of a family of geometrically interlocking space-filling shapes, which we call woven tiles. Our framework is based on a unique combination of (1) Voronoi partitioning of space using curve segments as the Voronoi sites and (2) the design of these curve segments based on weave patterns closed under symmetry operations. The underlying weave geometry provides an interlocking property to the tiles and the closure property under symmetry operations ensure single tile can fill space. In order to demonstrate this general framework, we focus on specific symmetry operations induced by fabric weaving patterns. We specifically showcase the design and fabrication of woven tiles on flat and curved domains by using the most common 2-fold fabrics, namely, plain, twill, and satin weaves. We further evaluate and compare the mechanical behavior of the so created woven tiles through finite element analysis.

Index Terms—Space-Filling shapes, 3D Tile Design, Geometric interlocking, Fabric Weave, 3D printing, Computational Fabrication.

1 Introduction

1.1 Motivation

Space-filling shapes have applications in a wide range of areas from chemistry and biology to engineering and architecture [1]. Using space-filling shapes, we can compose and decompose complicated shell and volume structures for design and architectural applications. Space-filling shapes that are also tileable, can be further provide an economical way for constructing structures because they can be mass-produced. Despite their practical importance, the variety of 2.5D and 3D space-filling tiles at our disposal are quite limited. The most commonly known and used space-filling shapes are usually regular prisms such as rectangular bricks since they are relatively easy to manufacture and are widely available. However, reliance on regular prisms, significantly constrains our design space for obtaining reliable and robust structures.

A recent approach provides a conceptual framework for a systematic design of modular and tileable identical building blocks by significantly extending design space with Delaunay Lofts [2], and generalized Abeille tiles [3]. In this conceptual framework, the higher-dimensional Voronoi sites that are closed under symmetry operations are used to partition space. Using this framework, it has been possible produce identical space-filling modular building blocks to decompose planar shells such as Delaunay Lofts [2], and generalized Abeille tiles [3]. One problem with Delaunay and generalized Abeille tiles is that they are only topologically interlocking [4], [5]. In other words, while these tiles are assembled simply by placing them next to each other and therefore cannot be constrained to **stay together** without using a peripheral force. In this paper, we present a new approach for ***geometrically interlocked tiling***.

This paper is an extension of our recently published work on bi-axial woven tiles [6] where we utilized the symmetry of fabric weaves to achieve geometric interlocking. Specifically, we demonstrate the decomposition of curved domains into geometrically interlocked space-filling components and also show that our tiled assemblies are significantly stronger than their monolithic counterparts.

1.2 Geometric Interlocking

Given an assembly of objects embedded in a given space, we call the objects geometrically interlocked with each other if is it impossible to assemble or disassemble them without applying at least one or more of the following operations: (1) lifting at the objects up into a higher dimensional space, (2) deforming at least one object (i.e. applying a non-rigid transformation), and (3) cutting at least one object into at least two or more parts. Two relatively obvious examples that exhibit such a behaviour are a pair of links in a chain or a box inside another box. However, we show that there is a vast space of shapes that is not only geometrically interlocking but also space-filling. As a more relevant example, consider a simple jig-saw puzzle embedded in 2-space. In order to assemble this puzzle together using only rigid transformation the only choice is to lift the pieces up into 3-space and put them back on the plane. If the movement of the pieces is restricted to 2-space then the only way to assemble this puzzle would be to either deform at least one piece so as to fit it between two other pieces or to cut at

- *V. R. Krishnamurthy is are with J. Mike Walker '66 Department of Mechanical Engineering and Department of Computer Science and Engineering (by Affiliation), Texas A&M University, College Station, USA. E-mail: vinayak@tamu.edu*
- *E. Akleman is with the Department of Visualization and Department of Computer Science and Engineering (by Affiliation), Texas A&M University, College Station, USA. E-mail: ergun.akleman@gmail.com*
- *S. G. Subramanian and M. Ebert are with J. Mike Walker '66 Department of Mechanical Engineering, Texas A&M University, College Station, USA. E-mail: sai3097ganesh@tamu.edu; matt_ebert@tamu.edu*
- *J. Cui, C. Fu, and C. Starrett are with the Department of Visualization, Texas A&M University, College Station, USA. E-mail: jiaqi96@tamu.edu; sqree@tamu.edu; cstarrett@tamu.edu*

Manuscript received Month XX, 2020; revised Month YY, 2020.

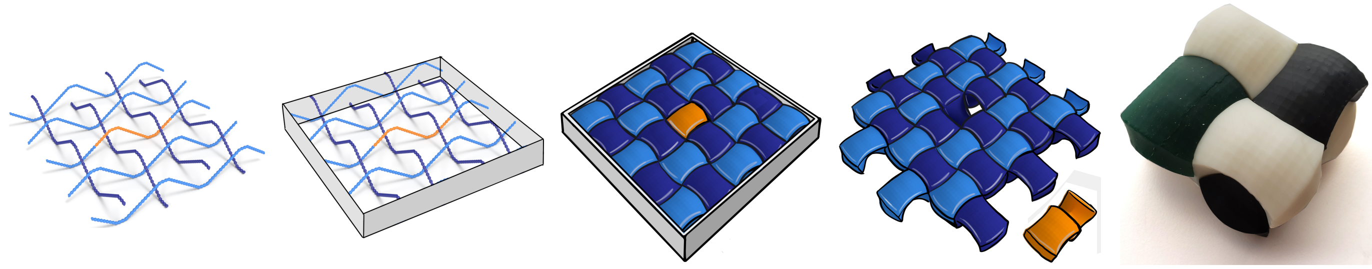

(a) *A set of curve segments that are closed under symmetry operations. The yellow curve shows the basic element of the repeating curve segment for this case.*

(b) *The curve segments in a 2.5D fundamental domain, which is rectangular prism.*

(c) *Voronoi decomposition of fundamental domain using curve segments as Voronoi sites. Yellow tile in the center is a space filling tile.*

(d) *Assembly of space filling tiles by its replicas. The yellow tile is removed to show the inner structure.*

(e) *Physical assembly of 3D printed tiles in a different configuration, where flexible dark green piece plays the role of locking this configuration.*

Fig. 1: *The computational pipeline for the geometric design and fabrication of woven tiles is shown. This particular example illustrates the tiles generated using the plain weave symmetries filling 2.5D space. The Figure 1c shows the curves in fundamental domain. The yellow curve shows the basic element of the repeating curve segment. All other curve segments in the fundamental domain can be obtained by rotating and translating this yellow curve. The Figure 1d shows overall assembly by removing the tile that corresponds to yellow curve. We obtained the shapes of top surfaces also with Voronoi decomposition.*

least one piece into at least two or more pieces so that one may use 2D rigid transformations (two translations and one rotation) to put them in place.

Interlocking objects have been extensively studied in several domains of science and engineering including mechanics, architecture, and computer graphics. For example, seminal works by Song et al. show several interesting applications for interlocking shapes including recursive puzzles [7], 3D printing [8] and reconfigurable furniture [9]. Many of these and several other works [10], [11], [12], [13] are based on the principle of a "**key**" element that holds the other parts in place in conjunction with other kinematic inter-dependencies. In spirit, these are conceptually similar to the so called topological interlocking shapes where the key actually facilitates the peripheral force necessary to hold other pieces together. We also found an interesting concept for interactive surface design with interlocking elements by Skouras et al. [14] that demonstrated geometric interlocking wherein they lock flexible elements through deformation. In this work, we specifically focus on ***geometric*** interlocking as a complementary idea to topological interlocking that has been widely explored in graphics and other domains.

1.3 Inspiration & Rationale

Our inspiration for geometric interlocking comes from the topological concept of *links*, which are equivalent to multiple interlocked circles embedded in 3D space. Links are generalized forms of knots, which are equivalent to a singe circle embedded in 3D space. We observe that using links as Voronoi sites to decompose a given volumetric domain automatically results in geometrically interlocked space-filling partitioning of the domain. An efficient approach of modeling links is embedding multi-circles onto discretized surfaces (polygonal meshes) using extended graph rotation systems [15]. Such an approach can be implemented by labeling each edge of a given polygonal mesh using an integer. Particularly, if the labeling is binary (i.e. every edge is labeled either 1 or 0) the result is guaranteed to be either an alternating link [16] or an alternating knot [17]. In both cases, we obtain what is commonly known as a plain woven object. One problem with this general approach is that it is theoretically impossible to obtain weave equivalent structures (such as twill and satin) other that plain weaves (alternating links) unless we restrict the polygonal mesh topology in a specific manner [18], [19]. Although such mesh topologies have been shown to exist [20], [21], [22], [23], there is currently no systematic and simple way for producing regular links on regular meshes except $(4, 4, 1)$, that is, a regular quadrilateral grid wherein every face is a quadrilateral and every vertex has a valency of four.

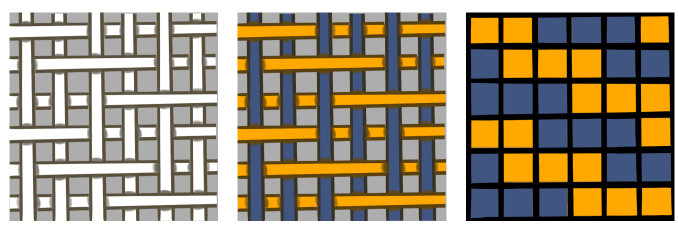

(a) *Top view of a weave with uncolored threads.*

(b) *Same weave with colored warp and weft threads.*

(c) *Matrix view of the same weave.*

Fig. 2: The fundamental domain of 2-way 2-fold fabrics is a rectangle and they can be represented as a simple matrix. The warp threads are colored blue and weft threads are colored yellow to differentiate the two threads in the final matrix.

Our approach leverages woven objects based on $(4, 4, 1)$ regular meshes, which incidentally, are the commonly known woven fabrics, fabric weaves or 2-fold 2-way fabrics as catalogued by Grünbaum and Shephard [24]. Here, "2-*way*" means that these fabrics are manufactured using two sets of interlacing strands, called warp and weft, at right angles to each other (see Figure 2a). The word 2-fold means there are never more than two strands crossing each other [16]. Given the focus on geometric interlocking, our main challenge was to identify a design space of weaves that covers a large variety of patterns and is simultaneously simple to identify and classify.

To address this challenge, we note that fabric weaves can be viewed as matrices (Figure 2). In fact, the seminal studies [24], [25], [26], [27] on the mathematical properties of fabric weaves used this representation to catalogue fabric weaves. For instance, the most widely used fabric weaves, namely, genus-1 2-fold 2-way fabrics can simply be constructed by shifting each row in the matrix by c units to the right for some fixed value of the parameter c (Figure 2). In fact, these genus-1 fabrics include the three most well known fabrics, namely, plain, twill, and satin that can be represented as a triplet $[a, b, c]$ where each row with length n consists of a number of consecutive weft threads and $b = n - b$ number of consecutive warp threads (Figure 3a). More importantly, Grünbaum and Shephard further showed that [27] he $[a, b, c]$-fabrics are guaranteed to "*hang together*" if $n = a + b$ and c's are relatively prime. **We presently constrain our exploration with respect to this property it will guarantee geometric interlocking of the tiles resulting from the Voronoi partitioning. Note that the converse may not necessarily be true, i.e., not all geometrically interlocking structures may necessarily correspond to weaves that hang together. This needs to be studied further and is out of scope of this paper.**

The genus-1 isonemal fabrics described by the $[a, b, c]$ notation not only include well-known patterns such as plain, twill, and satin but also a wide variety of additional bi-axial weaving patterns (Figure 3b). Among the $[a, b, c]$ patterns, the pattern is guaranteed to be rotation-invariant for plain, twill, and satin cases. This is because in plain, twill, and satin cases, warp and weft patterns are mirrored versions of each other [24]. Since our goal is to obtain a single tile, we focus on only plain, twill and satin woven tiles in this paper. Plain, twill and satin fabric weaves are also known that they can form strong interlocked structures that can stay together without a need for external forces [28]. This particular $[a, b, c]$ characterization, therefore, simplifies the problem of classifying and analyzing fabric weaves thereby providing a simple yet powerful means for exposing a large design space of geometrically interlocking tiles.

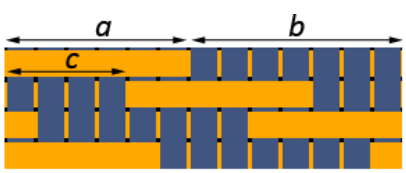

(a) Three parameters, a, b and, c, are sufficient to define all of the important 2-fold, 2-way genus-1 fabrics

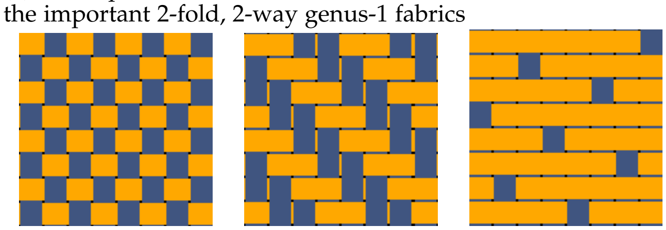

Plain: $[1, 1, 1]$ Twill: $[2, 2, 1]$ Twill: $[7, 1, 3]$

(b) Examples of isonemal genus-1 patterns that can be represented by three parameters shown in Figure 3a.

Using these properties of the fabric weaves as our rationale, we investigate constructing tiled assemblies of geometrically interlocking space-filling shapes that leverage the thread interlacing process from plain, twill and satin woven fabrics.

1.4 Summary of Approach

Using the properties of plain, twill and satin woven fabrics, our approach is to obtain desired curves segments that are closed under symmetry operations (i.e. applying rigid transformations results in another curve segment that belongs to the weave). One simplification of these fabrics is that each curve segment can be chosen to be planar. In addition, we can define all plain, twill and satin fabric patterns using only three parameters. For example, for a 2-way genus-1 weave pattern such as a plain weave (Figure 1a), we can simply embed it in a fundamental domain shaped as a prism with a square base (Figure 1b). Subsequently, all we need to do is compute Voronoi decomposition of the fundamental domain (Figure 1c) resulting in a set of identical space-filling tiles (one tile shown as yellow in Figures 1c and 1d).

We present a simple method to compute Voronoi decomposition of fundamental domain with these curve segments. We first sample each curve segment to obtain a piece-wise linear approximation. We compute 3D Voronoi decomposition for each sample point. This process gives us a set of convex Voronoi polyhedra for the same curve segment. The union of these convex polyhedra gives us desired space filling tile. We identify simple and robust algorithms to take union of all convex Voronoi polyhedra that comes from the same piece-wise linear curve segment. We also developed a tile beautification process inspired by the fact that the points of equal distance to a planar surface and a line parallel to the surface lie on a parabolic cylinder. We add two planar surfaces that sandwich the control curves from top and bottom also as Voronoi sites. Resulting Voronoi decomposition automatically provides nice boundaries comprised of parabolic regions.

To demonstrate our approach, we designed, numerically analyzed, and fabricated several varieties of woven tiles. Because of their symmetry properties, these tiles can be assembled in more than a single configuration. Some assembly structures can even create loops as shown in Figure 1e. For these cases, we have shown that it is possible to lock the pieces using one flexible piece.

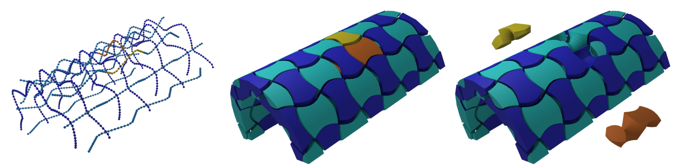

(a) *Initial curves. Each curve consists of four segments.* (b) *Decomposition obtained by original curves in 4a.* (c) *Exploded view showing two types of woven tiles.*

Fig. 4: *The decompositions of half-cylindrical shell using plain woven tiles.*

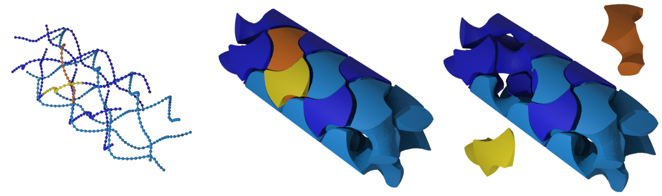

(a) *Initial curves. Each curve consists of four segments.* (b) *Decomposition obtained by original curves in 5a.* (c) *Exploded view showing two types of woven tiles.*

Fig. 5: *The decomposition of half-cylindrical shell using plain woven tiles.*

1.5 Our Contributions

Our overarching contribution in this work is a general conceptual framework for generating space-filling and interlocking tiles based on the fundamental principles of fabric weave patterns in conjunction with space decomposition using 3D Voronoi partition. Based on this framework, we make four specific contributions as listed below:

1) We use our general framework to develop a simple and intuitive methodology for the design and construct *woven tiles*, space-filling tiles derived from the symmetries induced by woven fabrics.
2) We introduce a simple and effective algorithm for approximating the Voronoi decomposition of space with labelled curve segments as the Voronoi sites. The algorithm uses a simple process that first discretizes a curve segment into a sequence of points and then constructs a Voronoi cell of the curve simply by computing the union of *constitutive* Voronoi cells for each point on the curve.
3) We systematically study our approach by generating several cases of *woven tiles* on flat as well as curved domains. We also demonstrate techniques for the fabrication and assembly these tiles for the flat domain with a variety of materials (plastic, wax, and metal) by using different 3D printing, molding, and casting techniques. Furthermore, we demonstrate that these tiles can be assembled more than single configuration. From the same group, it is even possible to obtain two assemblies with different chirality (i.e. mirrored versions of each other).
4) Finally, we present a comprehensive structural evaluation of plain, twill, and satin tile assemblies for different domain shapes including flat, cylindrical, bi-quadratic, and saddle. The finite element failure analyses of these assemblies showed that our assemblies allow for localizing failure. This strongly reinforces the idea of toughening by fragmentation in mechanics literature [4].

1.5.1 Extended Work:

In this extended version of our previously published work [6], we demonstrate the application of our approach on non-planar fundamental domains, specifically half and full cylinders (Figures 4 and 5 respectively), for each of the three weave patterns (plain, twill, and satin). The cylindrical case, unlike our previous planar examples, exposed a new relationship between the alignment of the Voronoi sites (i.e. weave curves) relative to the principal curvature directions of the domain and chirality of the resulting woven tiles. This extension to cylindrical surfaces also sheds light on the potential relationship between principal curvature and the number of distinct tiles possible (Section 4.4). We have also extended the work to curved domains that are homomorphic to rectangular prisms. These domains are defined by using height functions and they may not necessarily be fundamental domain. Therefore, we do not necessarily have single tile solutions. To achieve this, we further extended our original space decomposition algorithm from [6] to handle curved domains (section 3.3). We systematically study the effect of different geometric features through examples of curved domains (section 4.1). We present a completely new FEA analysis (Section 5) to assess the amount of load to cause failure in our assemblies for flat as well as several curved domains. Our results (the maximum force needed to cause failure) with respect to the ground truth (a monolithic structure) demonstrate the viability of our approach for some future applications to design and manufacturing.

2 Related Work

History is rich with examples of puzzle-like interlocking structures, which is analyzed under the names such as stereotomy [29], [30], [31], Leonardo grids or nexorades [32], [33], [34] and topological interlocking [4], [35], [36], [37]. One of the most remarkable examples of interlocking structures is the Abeille flat vault, which is designed by French architect and engineer Joseph Abeille [3], [38], [39]. Our work is similar to Leonardo grids, which are also called the nexorades, are types of structures that are constructed using notched rods that fit into the notches of adjacent rods resembling fabric weaves [40], [41]. Unlike Leonardo grids, our structures are also space filling. In other words, their assemblies forms decomposed monolithic blocks.

Space filling polyhedra, which can be used to tessellate (or decompose) a space [24], are defined as a cellular structure whose replicas together can fill all of space watertight, i.e. without having any voids between them [1]. While 2D tessellations and 2D space filling tiles are well-understood [24], problems related to 2.5D and 3D tessellations and tiles (i.e. shell and volume structures respectively) are still perceived as difficult. It appears that Delaunay's original intention for the use of Delaunay diagrams was to obtain space filling polyhedra using points that are closed under symmetry operation as Voronoi sites, which he called Stereohedra [42], [43]. As mentioned earlier, recent work on Delaunay Lofts and Generalized Abeille Tiles use higher dimensional Voronoi sites to obtain more complicated space filling structures [2], [3]. Allowing any type of shapes as Voronoi sites not only enables a systematic search of desired shapes from large number of potential candidates, but also provides **a simple design methodology** to construct space filling structures.

Based on this point of view, the key parameters for the classification of space-filling shapes are essentially the topological and geometric properties of Voronoi sites and their overall arrangements that are usually be obtained by symmetry transformations (rotation, translation, and mirror operations). The types of shapes and transformations uniquely determine the properties of the space decomposition. Now, based on this view point, let us again look at Stereohedra, Delaunay lofts and generalized Abeille tiles.

For Stereohedra, the shapes of Voronoi sites are points, 3D L_2 norm is used for distance computation, underlying space is 3D and any symmetry operation in 3D are allowed [42], [43]. Based on these properties, we conclude that Stereohedra can theoretically represent every convex space filling polyhedra in 3D. Since the points are used as Voronoi sites and L_2 norm is used, the faces must be planar and edges must be straight in the resulting Voronoi decomposition of the 3D space.

For Delaunay lofts, on the other hand, the shapes of Voronoi sites are curves that are given in the form of $x = f(z)$ and $y = g(z)$, for every planar layer $z = c$ where c is a real constant, a 2D L_2 norm is used to compute distance, underlying space is 2.5 or 3D and only 17 wallpaper symmetries are allowed in every layer $z = c$ [2]. Based on these properties, we conclude that Delaunay lofts (1) consists of a stacked layers of planar convex polygons with straight edges, and (2) in each layer there can be only one convex polygon. In Delaunay lofts the number of sides of the stacked convex polygons can change from one layer to another. In conclusion, the faces of the Delaunay lofts are ruled surfaces since they consist of sweeping lines. Edges of the faces can be curved. For generalized Abeille tiles, Voronoi sites can be ruled surfaces or tree-structures, which can significantly extend design space [3]. However, they do not provide geometric interlocking property.

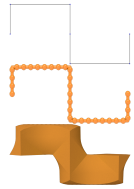

(a) *For* $[1,1,1]$.

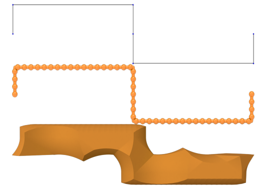

(b) *For* $[2,2,1]$ *twill weaving.*

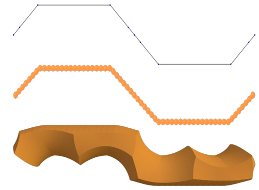

(c) *For* $[2,2,1]$ *twill weaving.*

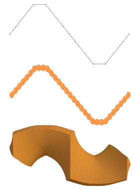

(d) *For* $[1,1,1]$.

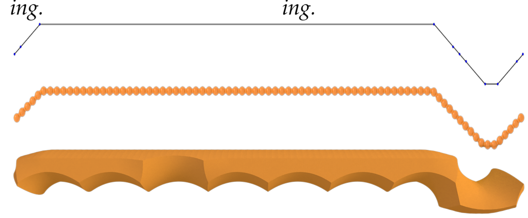

(e) *For* $[7,1,3]$ *satin weaving.*

Fig. 6: Examples of plain, twill and satin woven tiles obtained using basic degree-1 NURBS curves. Each curve is created by changing positions of 11 control points. The figures at the top are actual curves. The middle figures are points that are created by sampling the initial curves. These points that approximate the curves are used as Voronoi sites. The figures at the bottom are woven tiles that are created using sample points as Voronoi sites.

3 Design Modeling Methodology

For bi-axial woven tiles in this paper, the shapes of Voronoi sites are curve segments obtained by decomposing planar periodic curves that are given -essentially[1]- in the form of $z = F(x+n) = F(x)$ and $z = G(y+n) = G(y)$, where $n = a+b$ the period of fabric, where F can be any periodic function as far as it consists of a-length up regions and b-length down regions as shown in Figure 6. The function G is just the mirror of F with a-length down regions and b-length up regions. The curve segments are obtained from these two periodic functions by just restricting its domain into a region such as $(x_0, x_0 + kn]$. These curve segments are closed under symmetries of bi-axial weaving patterns, that are given by 90^0 rotation and translation operations. 3D L_2 norm is used for distance computation. Underlying space is normally 2.5D, i.e. a planar shell structure [44].

Based on these properties, it is clear that the resulting tiles would usually be genus-0 surfaces with curved faces and edges. Because of its bi-axial property, the fundamental domain for these tiles would always be a rectangular prism, an extruded version of the original rectangular fundamental domain of corresponding 2-way 2-fold fabric [45]. Therefore, the tiles that perfectly decompose this rectangular prism domain will also fill all 3D space. Our woven tile design process consists of three steps: (1) Designing curve segments; (2) Designing 3D configuration of the curves segments to be used as Voronoi sites; and (3) Decomposition of the space using Voronoi tessellation. For all steps, we have used the simplest approaches which simplify the design process and provides robust computation.

1. We actually use parametric curves. This is only for providing a quick and simple explanation without a loss of generality

3.1 Designing Curve Segments

We designed our control curves by using Non-Uniform Rational B-Splines (NURBS). We initially allowed the higher degree curves to allow C^1 and C^2 continuity, but, quickly realized that piecewise-linear curves are sufficient to obtain desired results for bi-axial woven tiles. Therefore, we designed all curves with degree-1 NURBS. For all cases, we use the same 11 control points. We simply move the positions of the control points to obtain the curve segments for desired weaving pattern as shown in Figure 6. To construct these curves, in addition to three weaving parameters, i.e. a, b, and c, we provide one additional control: the angle of connection of two consecutive tiles. By changing the angle we can obtain **Square Waves**, which appears to be binary function such as the ones shown in Figures 6a and 6b, and **Partly Triangular Waves**, which appears to be regular piece-wise linear such as the ones shown Figures 6d, 6c and 6e. The two consecutive tiles produced by square waves can sit at the top of each other as shown in Figures 6a and 6b. With partly triangular tiles, we can adjust this angle as shown in Figures 6d and 6c and 6e.

3.2 Designing Voronoi Sites

Based on three weaving parameters, i.e. a, b, and c, we have developed an interface to create 3D curve segments that are closed under symmetry operations of 2-fold 2-way genus-1 fabrics. The algorithm consists of three stages as follows:

1) Create initial curve segment as $x = F_x(t)$, $y = 0$ and $z = F_z(t)$ based on a and b values, and curve type. Without loss of generalization, assume $t \in [0,1]$, $z \in [0,1]$, and $x \in [-n/2, n/2]$. Note that $n = a + b = F_x(1) - F_x(0)$.
2) Create two replicas of the curve and translate them along the x axis by adding and subtracting its period $n = a + b$

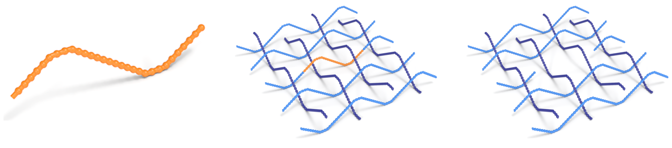

(a) *Basic curve segment in 3D for* $[1, 1, 1]$ *plain weaving.*

(b) *Overall configuration for decomposition of rectangular prism domain.*

(c) *Union of surrounding curves provides mold structure.*

Fig. 7: An example for designing control curves for $[1, 1, 1]$ plain woven tiles.

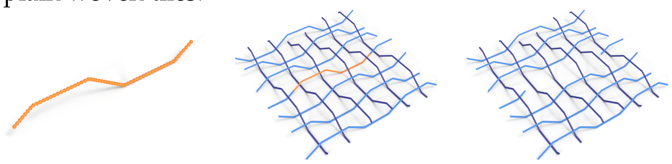

(a) *Basic curve segment in 3D for* $[2, 2, 1]$ *twill woven tiles.*

(b) *Overall configuration for decomposition of rectangular prism domain.*

(c) *Union of surrounding curves provides mold structure.*

Fig. 8: An example for designing control curves for $[2, 2, 1]$ twill woven tiles.

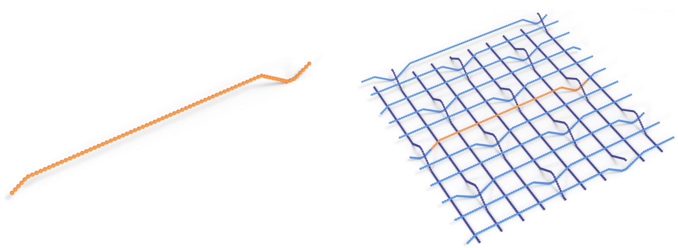

(a) *Basic curve segment in 3D for* $[7, 1, 3]$ *satin woven tiles.*

(b) *Overall configuration for decomposition of rectangular prism domain.*

Fig. 9: An example for designing control curves for $[7, 1, 3]$ satin woven tiles.

respectively. This creates three copies of initial curve that follows each other.

3) Create two replicas of of these three curves. Translate one of them using $(c, 1, 0)$ vector and translate the other $(-c, -1, 0)$. This translation operation must be done in modulo $3n$.
   - **Remark 1:** This operation creates a $3n \times 2 \times 1$ rectangular prism domain, which is sufficient to compute tiles. Note that we assume the height of the curves is 1 unit.
   - **Remark 2:** This rectangular domain is not a fundamental domain of the curve symmetries. It is only applicable for genus-1 case.
4) Create perpendicular curve segments.
5) **Remark 3:** Perpendicular curve segments are guaranteed to be the same for plain, twill and satin. Therefore, we only focus on these to obtain single tile.

In practice we create these curves in a larger rectangular domain as shown in Figures 7, 8, and 9 to see the structure of the curves better. These rectangular domains must be larger than the $3n \times 2 \times 1$ domain we described earlier to guarantee we obtain at least one tile that can fill the space. In other words, at least one curve must be covered with its neighboring curves to guarantee that the Voronoi region that corresponds that particular curve segment fill the space. In Figures 7, 8, and 9, which shows two plain, two twill and one satin cases, the center curve is colored yellow. We have implemented this interface by using SideFX's Houdini, which is a robust 3D software that provides a node-based system for fast and easy interface development.

3.3 Decomposition of the Space

Accurate decomposition of a given rectangular prism using continuous curves as Voronoi sites can be computationally complicated. We have developed a simple method that provides us reasonably good approximation of decomposition of domains using discrete approximation of the curves. We further extend our original algorithm [6] to handle domains that are homomorphic to rectangular prisms. Our algorithm consists of seven stages:

1) For a given weave symmetry, generate the control curves in the rectangular prism domain. Ensure that the control curves are completely immersed within the prism domain. This step is necessary to guarantee resulted Voronoi regions are connected.
2) Map the rectangular prism domain onto a desired domain and apply the mapping to the original control curves.
   - **Remark 0:** Since we ensured that our original curves were immersed in the rectangular prism domain, the mapped curves will naturally remain immersed in the desired domain thereby ensuring connected components.
3) Sample the control curves by obtaining the same number of points for each curve segment.
4) For (optional) beautification step, sample boundary of the domain and use it as an additional Voronoi site. In the case of plane sample two sandwiching (or bounding) planes. If not, skip this step. All the examples in this section are created using this step. However, none of the curved domain examples in section 4.1 use beautification step.
5) Label points as follows:
   - The points that are originated from the same curve are labeled using the same label, an integer larger than 0, say i.
   - **Remark 1:** If the beautification step is used, the points coming from bounding surface (the sandwiching planes in rectangular prism case) are labeled 0.
6) Decompose the space using 3D Voronoi of these points, which gives us a set of labeled Voronoi regions, which are labeled convex polyhedra.
7) Take union of all Voronoi regions with the same label to obtain desired space filling tiles. Union operation consists of only face removal operations as follows:
   - Remove the shared faces of two consecutive convex polyhedra coming from two consecutive sample points on the curve.
   - **Remark 2:** These faces will always have the same vertex positions with opposing order.
   - **Remark 3:** If underlying mesh data structure provides consistent information, this operation is guaranteed to

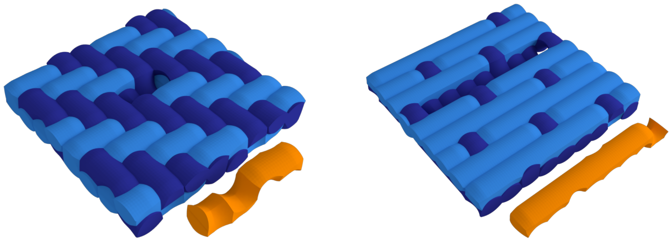

(a) *An assembly of twill,* $[2, 2, 1]$. (b) *An assembly of satin,* $[7, 1, 3]$.

Fig. 10: Examples of assemblies that show only the tiles cut to stay in rectangular domain.

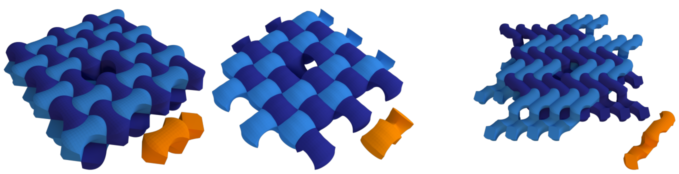

(a) $[1, 1, 1]$. (b) $[1, 1, 1]$ *tile.* (c) *A twill,* $[2, 2, 1]$, *woven tile.*

Fig. 11: Examples of assemblies with uncut tiles .

provide a 2-manifold mesh. Even if the underlying data structure does not provide consistent information, the operation creates a disconnected set of polygons that can still be 3D printed using an STL file.

- **Remark 4:** If beautification step is used, ignore polyhedra labeled 0, since those define the outside region.
- **Remark 5:** If the beautification step is skipped, i.e. boundary surface of the domain (two sandwiching planes in planar case) is not used as Voronoi site, take an intersection with the domain (with bounding rectangular prism for planar case). Stage 1 guarantees that intersection operation does not produce disconnected Voronoi regions.

We have implemented this stage in both in Matlab and Houdini. For 3D Voronoi decomposition of points, we used build in functions available in Matlab and Houdini.

4 Results: Geometric Evaluation

The geometry and topology of weaves has a rich research history with several open questions relating to the ability of the weaves to *hold together*. The works by Grunbaum et al. [24] assume that the threads being woven are infinitely long. This, obviously is not the case with woven tiles, making it more difficult to completely and formally characterize the assembly of woven tiles. Therefore, we have evaluated woven structures for two types of domains: (1) curved domains, and (2) planar domains. We evaluated both types of domains for three types common weaving patterns, namely plain, twill, and satin.

4.1 Woven Tiles on Curved Domains

We have shown earlier that woven tiles can be created in a planar domain with control curves designed directly based on the weave symmetry (Figures 10 and 11). To obtain curved domains, we directly extended this methodology by mapping the control curves onto domains that are homomorphic to rectangular prisms such as cylindrical shells or shells given by height fields, in the form of $f(x, y) - a \leq z \leq f(x, y) + a$, where a is a positive real number. To demonstrate this idea, we have created a variety of bi-axial woven structures with curved geometry (for examples see the four decomposed curved domains in Figure 12). In all of these four curved domains and 12 cases, we used mapped control curves as Voronoi sites to decompose given curved domains. All examples of bi-axial woven tiles in curved domains are created without beautification step.

The three cylinder cases, which are shown in Figures 12a, 12b, and 12c, are obtained by bending the plain, twill and satin control curves along a particular axis. This also provides = an example of zero Gaussian curvature with one non-zero principle curvature. For all the other cases, we used height fields. For bulging cases, which are shown in Figures 12d, 12e, and 12f, we used a bi-quadratic function $f(x, y) = (x+1)(x-1)(y+1)(y-1) = x^2y^2 - x - y + 1$. This makes the boundaries (that are formed by lines $x+1$, $x-1$, $y+1$ and $y-1$) to be fixed at $z = 0$ and the central region to have a positive Gaussian curvature. For the three concave-convex cases, which are shown in Figures 12g, 12h, and 12i, we used a combination of two bi-quadratic functions to show inflexion where the curvature transitions from positive to negative. For the three saddle cases, which are shown in Figures 12j, 12k, and 12l, we used a hyperbolic paraboloid function in the form of $z = x^2 - y^2$ to obtain a domain with negative Gaussian curvature with saddle at $x = y = 0$.

4.2 Woven Tiles in Planar Domains

For planar domains, our first evaluative step was to fabricate and physically assemble with the goal to explore how the symmetries induced by these patterns affect the method of creating assemblies of the respective tiles. We are particularly interested in two aspects of woven tile assembly: (a) locking ability which maps to the *holding-together* property of the weaves and (b) chiral configurations of woven tile assemblies.

All examples of bi-axial woven tiles in planar domain are created using beautification step. We have printed the tiles using both standard resin and elastic resin. For the purpose of investigation of various material properties and potential manufacturing options we made rubber molds of the tiles for casting silicon rubber and wax versions. The wax tiles were used to cast aluminum tiles via the lost wax casting process.

4.3 Locking Ability of Woven Tiles

The topology of a weaving pattern directly affects the locking ability of its corresponding woven tile. For instance, plain weave tiling results in self-locking configurations (Figure 13) identical to a plain woven fabric. Therefore, if zero tolerance is assumed, plain woven tiles cannot theoretically be assembled together with tiles constructed out of rigid materials such as PLA or Aluminium. In the 2×2 plain woven tile assembly shown in Figure 13a , one of the two black tiles (also the dark green tile in Figure 1e) is a compliant tile made of silicone, constructed through casting.

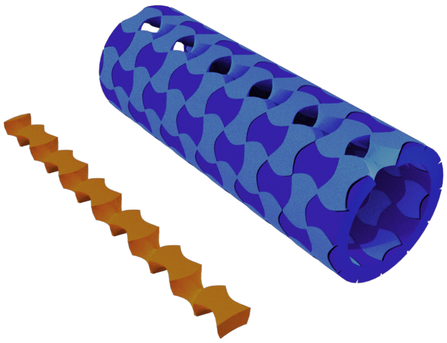

(a) *A cylindrical domain decomposed by bi-axial plain woven tiles.*

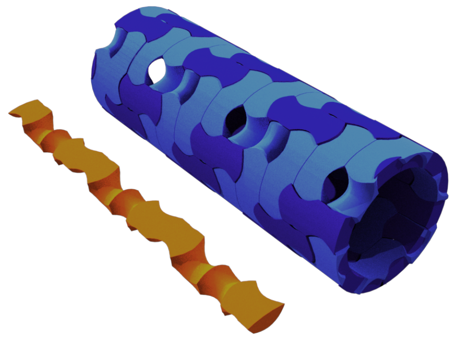

(b) *The same cylindrical domain decomposed by bi-axial twill woven tiles.*

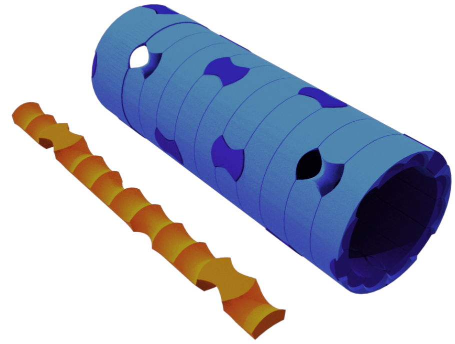

(c) *The same cylindrical domain decomposed by bi-axial satin woven tiles.*

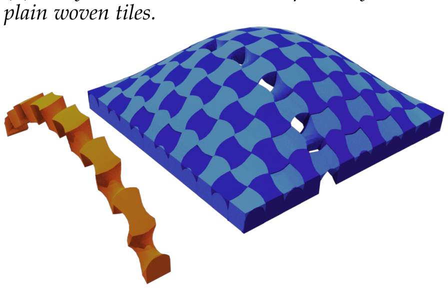

(d) *A bi-quadratic domain decomposed by bi-axial plain woven tiles.*

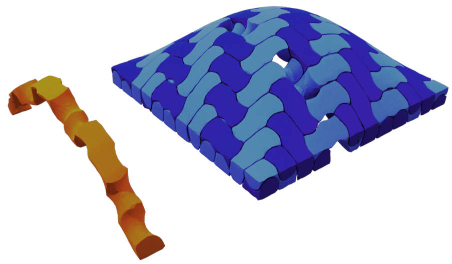

(e) *The same bi-quadratic domain decomposed by bi-axial twill woven tiles.*

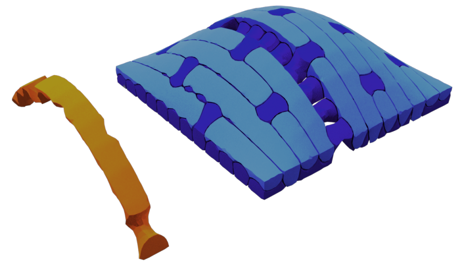

(f) *The same bi-quadratic domain decomposed by bi-axial satin woven tiles.*

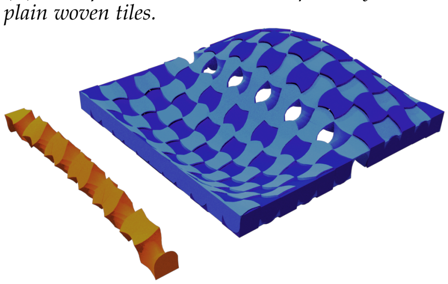

(g) *A concave-convex domain decomposed by bi-axial plain woven tiles.*

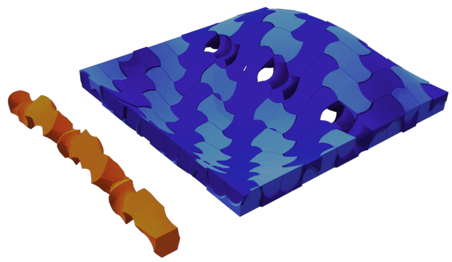

(h) *The same domain decomposed by bi-axial twill woven tiles.*

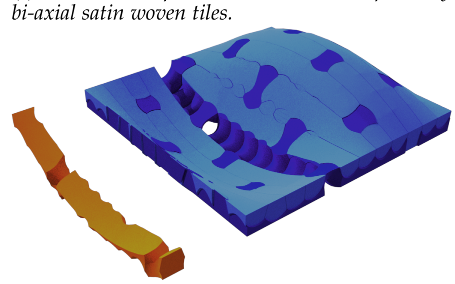

(i) *The same domain decomposed by bi-axial satin woven tiles.*

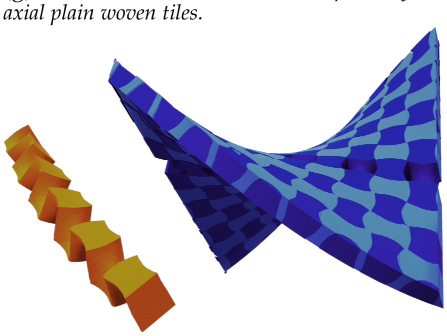

(j) *A saddle domain with maximum and minimum decomposed by bi-axial plain woven tiles.*

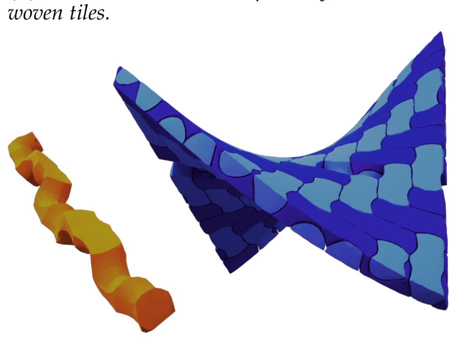

(k) *The same saddle domain decomposed by bi-axial twill woven tiles.*

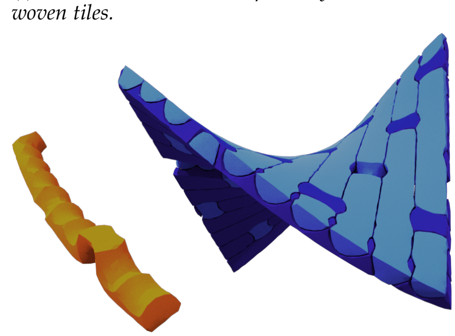

(l) *The same hyperbolic paraboloid domain decomposed by bi-axial satin woven tiles.*

Fig. 12: The curved domains that we have decomposed by using woven tiles. Note that in these decompositions, it is not possible to obtain single tile solution.

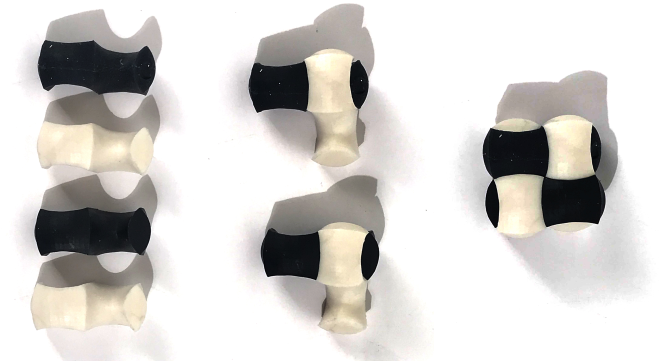

(a) *Individual plain tiles.* (b) *Plain tile pairs.* (c) *Complete assembly.*

Fig. 13: Assembly of plain woven tiles. One of the black pieces is a flexible silicone piece and is needed to successfully assemble plain tiles.

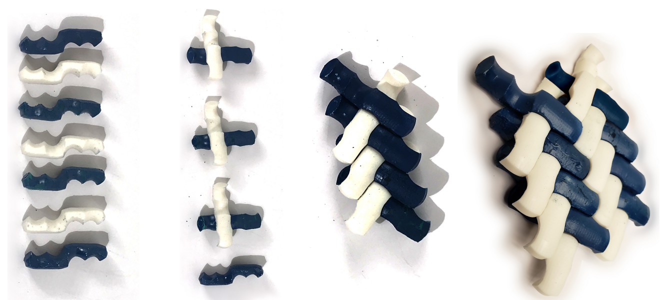

(a) *Individual twill tiles.* (b) *Twill pairs.* (c) *Twill assembly.* (d) *Twill assembly with one repetition.*

Fig. 14: Assembly of twill woven tiles.

(a) *Chiral pairs of plain woven tiles cannot be assembled.* (b) *Pairs belonging to the same chiral group can be assembled.* (c) *Plain woven assembly of two chiral groups.*

Fig. 16: An example of chirality in plain woven tiling of a flat domain.

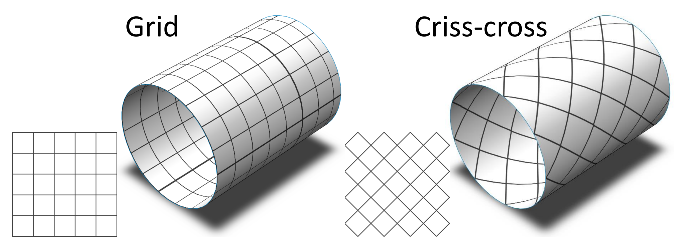

Fig. 17: Two parametrizations of the cylinder that were used to generate woven tiles. In case of the grid, we obtain two distinct tiles of different shapes (Figure 4). In case of criss-cross, we obtain two tiles that are chiral, i.e. mirror images of each other (Figure 5).

This assembly is structurally stable and the geometry of the elements itself holds the structure together. Specifically, both the assembly and disassembly of the plain woven tiling is possible only through the application of force. In addition to introducing a flexible element, we also experimented with all four pieces cast in wax as well as Aluminium. In this case, the shrinkage in the individual pieces allowed for the tiling to be assembled.

In case of twill weaves, we do not encounter the locking problem. As seen in Figure 14, the twill assembly can be simply created by an alternating placement of tiles along each of the axis (the white and blue tiles represent each axis). Therefore, neither the assembly nor disassembly require any application of force and we did not need any flexible pieces for twill (Figure 14c). There are two observations we make here. First, in the plain woven tiling, exactly half of each tile is above one adjacent tile and the other half is underneath a second adjacent tile. Second, in case of twill assembly, the unit tiles do share this alternate *above-underneath relationship* with their neighbors. However, note that if two twill woven tiles are combined to create a double-length tile (Figure 14d), we obtain the *above-underneath* relationship that will likely produce a perfectly interlocking tiling (thereby needing flexible tiles akin to the plain-woven case).

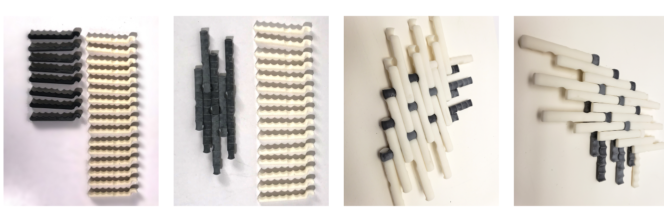

(a) *Individual satin tiles.* (b) *Lower assembly of satin tiles.* (c) *Complete satin assembly (view 1).* (d) *Complete satin assembly (view 2).*

Fig. 15: Assembly of satin woven tiles.

In case of satin weaves (Figure 15), we come to similar conclusions — there is a minimal number of repetitions of each tile to ensure a tightly packed interlocked assembly. While we can say for certain that the number of repetitions must be higher than twill, we currently do not claim what the number of repetitions should be. We believe that much work needs to be done in order to develop a formal theory for locking ability of woven tiles.

4.4 Chirality and Number of Distinct Tiles

A chiral object is one that is non-superposable on its mirror image. Chirality is a fundamental to several natural phenomena and engineering applications.Penne's work on planar layouts [46] provides a formal explanation to this property by connecting projective geometry and topology. We present two examples to explore the notion of chirality.

We also note that this notion may be linked to the number of *distinct* tiles for a given woven tiling of a domain.

Our first example that explores chirality is the plain-woven assembly wherein we observed that assembling the same plain-woven tiles in mirrored configurations leads to chiral assemblies (Figure 16). In this case, the individual tiles themselves are identical and chirality manifests itself on in the way these tiles are assembled. This, however, is not the case with our cylindrical cases (Figures 4 and 5).

In the cylindrical cases, we used two different ways of aligning the Voronoi sites (Figure 17): (1) grid along the principal curvature lines (along the axis and circumference as shown in Figure 4) and (2) criss-cross at a 45^o angle to the grid parametrization. In case of the grid, we obtain two distinct tiles of different shapes (Figure 4). The criss-cross parametrization results in a more interesting result. Here, we obtain two tiles that are chiral, i.e. mirror images of each other (Figure 5). This can be attributed to the mirror symmetry of the parameter lines and their lack of rotational invariance for the criss-cross case.

These observations indicate a deeper connection between surface parametrization, the number of distinct tiles, as well as chirality between the tiles. In fact, we conjecture that the only case when we will obtain a single unique space-filling tile is the planar domains because of zero-curvature and a rotationally invariant (4,4,1) grid parametrization.

5 RESULTS: STRUCTURAL EVALUATION

Our structural evaluation of woven tiles is based on the principle of **toughening by fragmentation** [37] that was originally utilized in the context of the mechanics of topological interlocking materials. The basic idea is that the toughness (the ability of a material to absorb energy and plastically deform without fracturing) of a monolithic material can be significantly enhanced if cracks are introduced strategically into the material. This is particularly relevant for us because our woven tile assemblies are space-filling, i.e. they consume the same volume as a monolithic block of the same geometry and dimensions. Therefore, our approach can be viewed as a means for fragmenting a monolithic solid at strategic locations as prescribed by the weave symmetries.

In order to understand whether our tiling could result in structurally better alternatives to monoliths, we conducted a series of Finite Element Analyses (FEA). Our specific objectives were to (1) measure the maximum amount of force before failure in our tiled assemblies in comparison with and (2) to measure the average stresses for the maximum load so as to better understand long term global failure as well. Finally, we also wanted to characterize the behaviour of different weave patterns for a given domain. To achieve these objectives, we conducted failure analysis on four different types of shapes, namely, flat, saddle, half-cylinder, and bi-quadratic across the three weave patterns (plain, twill, and satin).

5.1 Assumptions & Preparation

We used the assemblies generated using our extended algorithm (Figure 12) in our analysis. Note that the thickness of the domain is kept consistent across all geometries. We also generated a monolithic geometry for each of the domains that we explored. The dimensions for a given domain across the weave patterns was also made identical for fair comparison. All the peripheral boundaries of every tiled assembly was fixed to the ground. In our analyses, we used structured steel as the material of choice for a simple reason that it is ductile, follows Hooke's law (exhibits linear elasticy before plastic deformation). The values of assumed Young's Modulus is $2e+11$ Pa, Poisson's Ratio is 0.3, Bulk Modulus $1.6667e+11$ Pa, Shear Modulus $7.6923e+10$ Pa and Yield Strength is $2.5e+08$ Pa.

All the geometric modeling and pre-processing of the assembly were performed in Houdini FX 18.0.566. For each of the individual geometries obtained from the Voronoi decomposition for the thread of control curves, two operations were performed to prepare the assembly for simulation. One, the mesh is offset by a very small amount (about 0.001 units) to ensure that there are no self intersections. Two, the geometry is re-meshed to a specific target size, this process decreases file size and simulation time. All individual geometries are saved together in one STL file. This STL file is imported into SolidWorks 2020 to convert into a STEP file for simulation.

5.2 Evaluation Methodology

We used the ANSYS Workbench 2020 R1 for conducting the static structural analysis for all simulations. The STEP files were imported as solids into ANSYS and the tolerance setting identifies and creates contacts in between the geometries. These contacts would serve as a means of transferring forces across the individual pieces. All contacts were assumed to be friction-less. This ensures the forces being transferred between adjacent tiles are purely due to geometry and not the friction forces.

Our main objective was to compare the force required to cause the local failure of the assembly. In our case, failure is defined as the condition when the maximum value of Von Mises stress at any given point on any of the elements of the assembly equals the yield strength of the given material (the stress at which the material undergoes plastic deformation). In order to simulate this condition for a given tiling, we started with a force of 1.0×10^6 N force and gradually increased the force until the maximum observed stress in the assembly reached the yield strength. The force and the values of the average stress, strain, and the location of the max stress region in the assembly were recorded for all the simulations (Table 1).

5.3 Key Findings

First and foremost, we observe that the maximum force before local failure is greater in the monolithic case regardless of domain and weave pattern (Table 1). This is expected since any fragmentation or crack in a monolithic solid is known to reduce the static structural strength. However, the stresses along the first and second principal directions (see Appendix) indicate a reasonably uniform (non-localized) distribution of loads across the woven tile assemblies. While not through direct evidence, this connects to the idea of toughening by fragmentation. Based on this, we suspect that

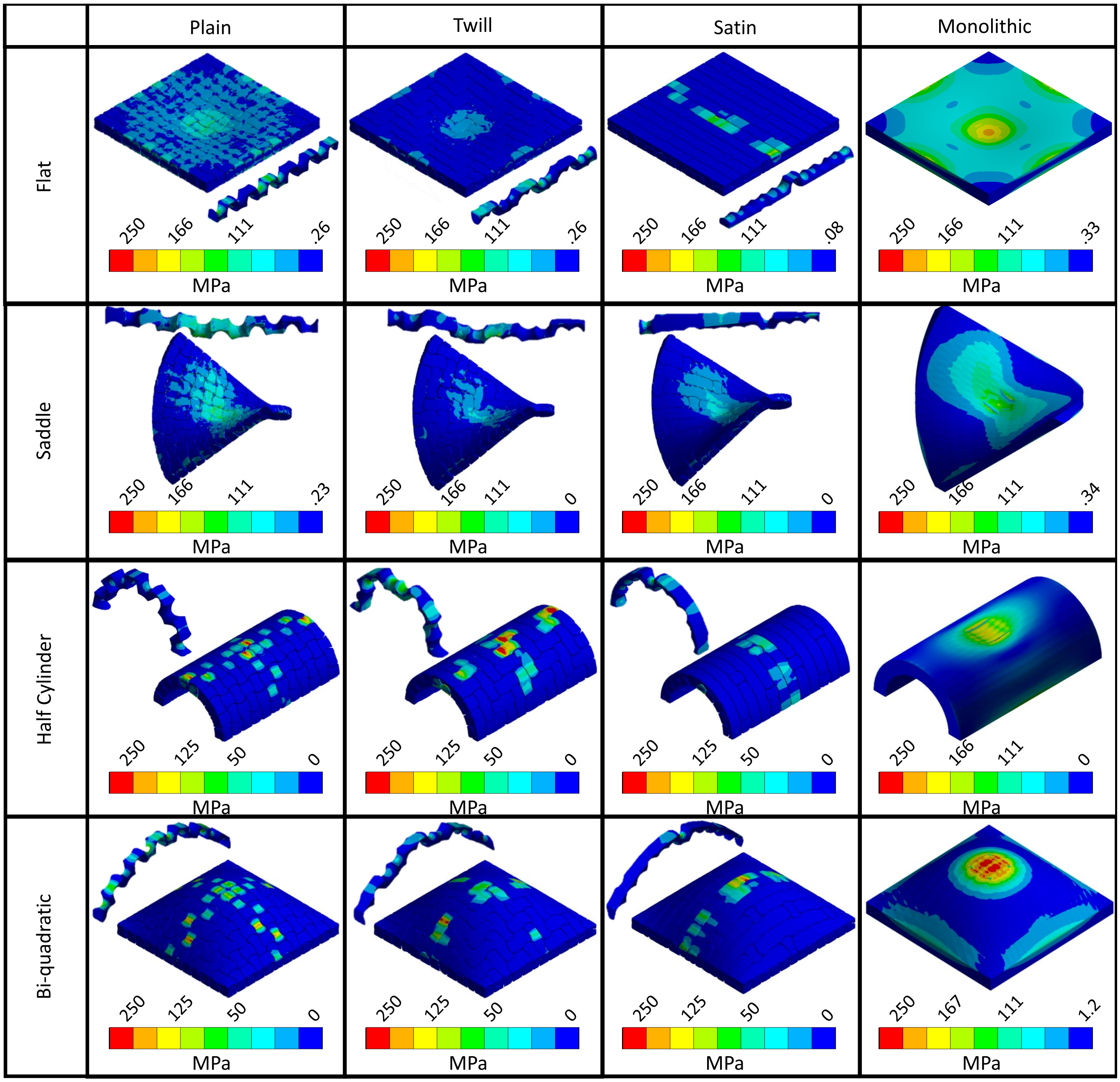

Fig. 18: Von-Mises stress distributions and deformation of assemblies of plain (left), twill (second to left), satin symmetries under normal loading compared with monolithic block of equivalent size. The assemblies are based on threads constructed out of multiple tiles. The first row shows for a flat case, the second has a deformed volume with a saddle point, the third is deformed to be a half cylinder, and the fourth is bi-quadratic. Each deformed volume contains assemblies of 12x12 cells except the half cylinder which has 10x12 cells.

	Flat				**Half-cylinder**			
	Plain	Twill	Satin	Monolithic	Plain	Twill	Satin	Monolithic
Max. Force. (N)	1.2×10^6	5.3×10^5	5.8×10^4	2.4×10^6	1.2×10^5	1.4×10^5	1.9×10^5	5.2×10^6
Avg. Sterss. (MPa)	26.9	12.9	3.3	47.8	4.3	5.2	4.6	42.00
Avg. Disp. (mm)	1.7×10^{-1}	8.1×10^{-2}	6.9×10^{-2}	2.1×10^{-2}	9.1×10^{-2}	9.3×10^{-2}	5.7×10^{-2}	6.8×10^{-2}
Max. Disp. (mm)	1.8	1.4	1.8	0.9	1.7	1.9	1.9	0.5
	Saddle				**Bi-quadratic**			
	Plain	Twill	Satin	Monolithic	Plain	Twill	Satin	Monolithic
Max. Force. (N)	2.2×10^6	1.1×10^6	1.5×10^5	2.9×10^6	1.7×10^5	1.2×10^5	1.2×10^5	5.5×10^6
Avg. Sterss. (MPa)	30.0	16.2	19.6	33.6	3.8	2.9	2.4	51.47
Avg. Disp. (mm)	1.8×10^{-1}	9.5×10^{-2}	1.1×10^{-1}	6.7×10^{-2}	3.9×10^{-2}	3.5×10^{-2}	2.2×10^{-2}	9.3×10^{-2}
Max. Disp. (mm)	1.7	1.3	1.6	0.4	0.7	0.8	0.7	0.70

TABLE 1: This tables lists the maximum load before failure, average stresses and displacements, and maximum displacements for different domains and weave patterns.

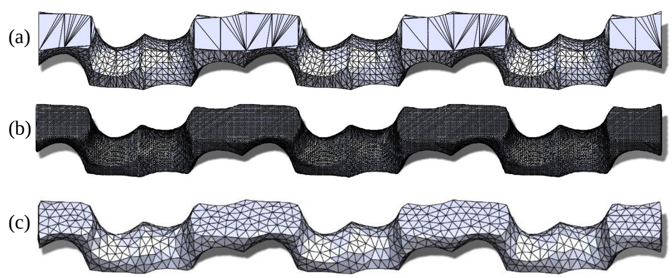

Fig. 19: These are the steps involved in pre-processing the threads for doing Finite Element Analysis. (a) is the thread that is obtained from the Voronoi decomposition, (b) is the mesh after offsetting the body to obtain a isosurface and (c) is the final output mesh that we obtain by remeshing the mesh from offset

woven tiles will be good candidates for applications that require energy absorption.

We observe some interesting dependencies of the force required for failure and the curvature of the domain as well as the type of weave. In case of flat and saddle geometries (i.e., curvature ≤ 0), plain weaves permit the highest value of force needed for failure (1.2×10^6 N for flat and 2.2×10^6 N for saddle). Not only that, the forces are also closest to the monolithic case when compared to other weaves indicating higher structural strength of plain weaves. In case of the cylinder and bi-quadratic domains (i.e., strictly positive curvature), woven tiles have notably lower structural strength. It is interesting to see that satin weaves permit highest force for failure in case of half-cylinder when compared with plain and twill. We also note that the magnitude of average stress induced is higher for the monolithic case across all domains and weaves. This is because the monolith case allows force to dissipate through the whole material while the weaves only transfer force through the threads interaction with other threads.

For a given domain, we did not observe much difference (relatively) in the maximum force before failure across different weave patterns. Even so, of all the domains, the bi-quadratic domain captured this property particularly well with the least amount of variation across weaves. In fact it also exhibits the least average stress (3.8 MPa) followed by the half-cylinder (4.3 MPa). Based on the geometry of the domain, that was expected.

A qualitative comparison of the stress distribution (Figure 18) clearly showed that the stresses were localized to only one or two threads that take the load completely regardless of the type of weave. However, we observe differences in how this localization occurs or different domains and weaves. Specifically, both plain and twill weaves distribute stress in a bi-directional manner (i.e. across two threads along different axes). On the other hand, satin predominantly exhibits a uni-directional distribution of stresses. What is also interesting to note is that plain tiling in the flat domain is, by, far, most similar to it's monolithic counterpart. This can be explained by a larger value of parameter a for satin — thus having more number of consecutive weft threads and restricting the potential transfer of forces to adjacent threads.

6 Discussion

The work presented in this paper provides (1) many new directions that need to be explored further; and (2) many interesting questions that need to investigated further. In the rest of this section, we discuss some of the future directions to explore and some of the questions to investigate.

6.1 Generalization based on Knots and Links

2-fold fabric structures are much richer than just 2-way genus-1 fabrics. Their real power can be best understood with extended graph rotation systems (EGRS) that was introduced in early 2010's [16], [47]. EGRS allows us to use orientable 2-manifold meshes as guide shapes to represent knots and links. The guide shapes help us to classify the fabrics. For instance, the guide shapes for 2-fold 2-way fabrics are regular grids embedded on genus-1 surfaces. For 2-fold 3-way fabrics, we need regular hexagonal or regular triangular grid embedded on genus-1 surfaces [16]. This is useful since some of the Leonardo grid designs are based on also 3-way woven patterns [41]. Using regular maps [22], [48], it is also possible to obtain hyperbolic tiling. Using the regular maps that correspond to hyperbolic tiles as guide shapes, 2-fold k-way genus-n fabrics can be obtained. From these fabrics, one can also obtain space filling shapes. For practical applications, there is a need for a significant amount theoretical work.

6.2 Application to Arbitrary Shapes

Extension of this work for arbitrary shapes is also possible using extended graph rotation systems (EGRS) [15]. Extended graph rotation systems provides a simple methodology to convert 2-manifold or 3-manifold mesh into knots in 3-space [16], [18], [47]. An advantage is that both shape of the curves and shape of the domain is fully defined by underlying polygonal mesh. Another advantage of this approach is that we can still obtain locally regular structures by applying subdivision schemes. This can help to reduce the number of distinct tiles. This particular generalization, moreover, can provide an extremely rich parameter space, which can, in turn make it harder to evaluate results. From this perspective, starting with bi-axial woven cases make sense since they provide a solid initial framework for preliminary analysis. As we have seen in this paper, even a relatively simple extension to curved domains that are homomorphic to rectangular prisms significantly extend the parameter space. However, from our preliminary explorations, several practical challenges (such as configuring the Voronoi sites within a shell domain, appropriate selection of shell thickness, etc.) need to be investigated further.

6.3 Locking

The key open question that we hope to answer in our future work is a formally supported computational methodology for determining minimum tile repetition to generate pure interlocking of woven tiles. Here, Dawson's work on the enumeration of weave families can provide an important starting point as a means to develop such a method based on sound mathematical principles. We see that the locking ability of woven tiles is related to three interlinked concepts in geometry and topology literature, namely, liftability [49], oriented matroids [50], and planar layouts of lines in 3-space [46]. To simply determine repetitions for locking is only the first step. Once we obtain a locking configuration, the second challenge is to determine the minimum number of flexible/compliant elements to make the assembly possible. We only showed this example for the plain woven tiles (Figure 1e). To the best of our knowledge, a general strategy for this problem is currently unavailable.

6.4 Mechanical Behavior & Topology

We observed that there is a correlation between the weave topology and the distribution of stresses across the interlocking elements of the assembly. A formal methodology for connecting the topology and structural properties is an important future direction that needs attention. As an important example, determining the relationship between direction of stress distributions to the weave parameters (the numbers a, b, and c in Figure 3a) will allow for systematic design of woven tiles for specific applications. Be that as it may, one of the most surprising results for us was the stark difference in the force required for failure in comparison to monolithic blocks. We believe a much deeper investigation is needed to understand why this happens such that we can generalize beyond this work to other structures constructed using other algorithms.

7 Conclusion & Future Directions

In this paper, we presented a methodology to design interlocking space-filling tiles that we call *woven tiles* that are generated using the topology of woven fabrics. To this end, we developed a method to create desired input curves segments using the properties of 2-fold 2-way genus-1 fabrics. We further developed a simple method to compute Voronoi decomposition of the curve segments. We demonstrated our general methodology by designing, fabricating, assembling, and mechanically analyzing woven tile assemblies. We 3D-printed some of these tiles and physically observed their mathematical and physical properties. We also developed molds to directly cast these shapes with a wider range of materials such as silicone and aluminium. While our physical evaluation of the individual and assembled properties of these tiles aligns with the current literature on woven fabrics, we show some interesting additional properties that were not previously apparent. Furthermore, our results suggest that interlocking these tiles have potential to replace existing extrusion based building blocks (such as bricks) which do not provide interlocking capability.

We want to point out that 2-fold fabrics are not really a final frontier. It is also possible to represent k-fold fabrics using 3-manifold meshes as guide shapes [47]. The extension to k-fold fabrics requires even more theoretical foundations, but it demonstrates the potential. A significant advantage of using guide shapes is that the topological properties of the knotted structures do not change with any geometric perturbation of the guide shapes. In conclusion, even though we chose our proof of concept tiles from 2-fold 2-way types, the ideas in this paper can be extended into more general types of fabrics with the maturation of theoretical work in regular maps and 3-manifold meshes.

Acknowledgments

This work was partially supported by the Texas A&M Engineering Experiment Station and the J. Mike Walker '66 Department of Mechanical Engineering at Texas A&M University, College Station. We would like to thank the reviewers for their valuable feedback. We would also like to thank Dr. Matt Pharr and Dr. Yuri Estrin for their advise on FEA-based failure analysis.

References

[1] A. L. Loeb, "Space-filling polyhedra," in *Space Structures*. NewYork, NY: Springer, 1991, pp. 127–132.

[2] S. G. Subramanian, M. Eng, V. R. Krishnamurthy, and E. Akleman, "Delaunay lofts: A biologically inspired approach for modeling space filling modular structures," *Computers & Graphics*, vol. 82, no. 8, pp. 73–83, 2019.

[3] E. Akleman, V. R. Krishnamurthy, C.-A. Fu, S. G. Subramanian, M. Ebert, M. Eng, C. Starrett, and H. Panchal, "Generalized abeille tiles: Topologically interlocked space-filling shapes generated based on fabric symmetries," *Computers & Graphics*, vol. 89, no. 8, pp. 156–166, 2020.

[4] Y. Estrin, A. Dyskin, and E. Pasternak, "Topological interlocking as a material design concept," *Materials Science and Engineering: C*, vol. 31, no. 6, pp. 1189–1194, 2011.

[5] Z. Wang, P. Song, F. Isvoranu, and M. Pauly, "Design and structural optimization of topological interlocking assemblies," *ACM Transactions on Graphics (TOG)*, vol. 38, no. 6, pp. 1–13, 2019.

[6] V. R. Krishnamurthy, E. Akleman, S. G. Subramanian, K. Boyd, C.-a. Fu, M. Ebert, C. Startett, and N. Yadav, "Bi-axial woven tiles: Interlocking space-filling shapes based on symmetries of bi-axial weaving patterns," in *Proceedings of the 46th graphics interface conference, GI*, 2020. [Online]. Available: https://openreview.net/forum?id=koAjrniDnBR

[7] P. Song, C.-W. Fu, and D. Cohen-Or, "Recursive interlocking puzzles," *ACM Transactions on Graphics (TOG)*, vol. 31, no. 6, pp. 1–10, 2012.

[8] P. Song, Z. Fu, L. Liu, and C.-W. Fu, "Printing 3d objects with interlocking parts," *Computer Aided Geometric Design*, vol. 35, pp. 137–148, 2015.

[9] P. Song, C.-W. Fu, Y. Jin, H. Xu, L. Liu, P.-A. Heng, and D. Cohen-Or, "Reconfigurable interlocking furniture," *ACM Transactions on Graphics (TOG)*, vol. 36, no. 6, pp. 1–14, 2017.

[10] Z. Wang, P. Song, and M. Pauly, "Desia: a general framework for designing interlocking assemblies," *ACM Transactions on Graphics (TOG)*, vol. 37, no. 6, pp. 1–14, 2018.

[11] N. Kita and K. Miyata, "Computational design of polyomino puzzles," *The Visual Computer*, pp. 1–11, 2020.

[12] C.-W. Fu, P. Song, X. Yan, L. W. Yang, P. K. Jayaraman, and D. Cohen-Or, "Computational interlocking furniture assembly," *ACM Transactions on Graphics (TOG)*, vol. 34, no. 4, pp. 1–11, 2015.

[13] S. Xin, C.-F. Lai, C.-W. Fu, T.-T. Wong, Y. He, and D. Cohen-Or, "Making burr puzzles from 3d models," *ACM Transactions on Graphics (TOG)*, vol. 30, no. 4, pp. 1–8, 2011.

[14] M. Skouras, S. Coros, E. Grinspun, and B. Thomaszewski, "Interactive surface design with interlocking elements," *ACM Transactions on Graphics (TOG)*, vol. 34, no. 6, pp. 1–7, 2015.

[15] E. Akleman, J. Chen, and J. L. Gross, "Extended graph rotation systems as a model for cyclic weaving on orientable surfaces," *Discrete Applied Mathematics*, vol. 193, pp. 61–79, 2015.

[16] E. Akleman, J. Chen, Q. Xing, and J. Gross, "Cyclic plain-weaving with extended graph rotation systems," *ACM Transactions on Graphics; Proceedings of SIGGRAPH'2009*, vol. 28, no. 3, pp. 78.1–78.8, August 2009.

[17] Q. Xing, E. Akleman, J. Chen, and J. L. Gross, "Single-cycle plain-woven objects," in *2010 Shape Modeling International Conference*. IEEE, 2010, pp. 90–99.

[18] E. Akleman, J. Chen, Y. Chen, Q. Xing, and J. L. Gross, "Cyclic twill-woven objects," *Computers & Graphics*, vol. 35, no. 3, pp. 623–631, 2011.

[19] S. Hu, Q. Xing, E. Akleman, J. Chen, and J. Gross, "Pattern mapping with quad-pattern-coverable quad-meshes," *Computers & Graphics*, vol. 36, no. 5, pp. 455–465, 2012.

[20] E. Akleman, V. Srinivasan, and E. Mandal, "Remeshing schemes for semi-regular tilings," in *Shape Modeling and Applications, 2005 International Conference*. IEEE, 2005, pp. 44–50.

[21] E. Akleman and J. Chen, "Regular mesh construction algorithms using regular handles," in *IEEE International Conference on Shape Modeling and Applications 2006 (SMI'06)*. IEEE, 2006, pp. 27–27.

[22] J. J. Van Wijk, "Symmetric tiling of closed surfaces: Visualization of regular maps," *ACM Transactions on Graphics (TOG)*, vol. 28, no. 3, p. 49, 2009.

[23] J. J. van Wijk, "Visualization of regular maps: The chase continues," *IEEE transactions on visualization and computer graphics*, vol. 20, no. 12, pp. 2614–2623, 2014.

[24] B. Grünbaum and G. C. Shephard, "Satins and twills: An introduction to the geometry of fabrics," *Mathematics Magazine*, vol. 53, no. 3, pp. 139–161, 1980.

[25] B. Grunbaum and G. C. Shephard, "A catalogue of isonemal fabrics," *Annals of the New York Academy of Sciences*, vol. 440, pp. 279–298, 1985.

[26] B. Grünbaum and G. C. Shephard, "An extension to the catalogue of isonemal fabrics," *Discrete Mathematics*, vol. 60, pp. 155–192, 1986. [Online]. Available: http://portal.acm.org/citation.cfm?id=10139.10148

[27] B. Grunbaum and G. C. Shephard, "Isonemal fabrics," *American Mathematical Monthly*, vol. 95, pp. 5–30, 1988.

[28] S.-P. Ng, K. J. Lau, and P. Tse, "3d finite element analysis of tensile notched strength of 2/2 twill weave fabric composites with drilled circular hole," *Composites Part B: Engineering*, vol. 31, no. 2, pp. 113–132, 2000.

[29] R. Evans, *The projective cast: architecture and its three geometries*. Cambridge, Mass: MIT press, 1995.

[30] G. Fallacara, "Toward a stereotomic design: Experimental constructions and didactic experiences," in *Proceedings of the Third International Congress on Construction History*. Chicago, IL: Construction History Society of America, 2009, pp. 553–560.

[31] S. Fernando, R. Saunders, and S. Weir, "Surveying stereotomy: Investigations in arches, vaults and digital stone masonry," in *Future of Architectural Research*. San Antonio, TX: Architectural Research Centers Consortium, 2015, p. 82.

[32] O. Baverel, H. Nooshin, Y. Kuroiwa, and G. Parke, "Nexorades," *International Journal of Space Structures*, vol. 15, no. 2, pp. 155–159, 2000.

[33] O. L. Baverel, "Nexorades: a family of interwoven space structures," Ph.D. dissertation, University of Surrey, 2000.

[34] C. Douthe and O. Baverel, "Design of nexorades or reciprocal frame systems with the dynamic relaxation method," *Computers & Structures*, vol. 87, no. 21, pp. 1296–1307, 2009.

[35] M. Weizmann, O. Amir, and Y. J. Grobman, "Topological interlocking in buildings: A case for the design and construction of floors," *Automation in Construction*, vol. 72, pp. 18–25, 2016.

[36] M. Carlesso, A. Molotnikov, T. Krause, K. Tushtev, S. Kroll, K. Rezwan, and Y. Estrin, "Enhancement of sound absorption properties using topologically interlocked elements," *Scripta Materialia*, vol. 66, no. 7, pp. 483–486, 2012.

[37] A. Dyskin, Y. Estrin, A. Kanel-Belov, and E. Pasternak, "A new concept in design of materials and structures: Assemblies of interlocked tetrahedron-shaped elements," *Scripta Materialia*, vol. 44, no. 12, pp. 2689–2694, 2001.

[38] O. Tessmann and M. Becker, "Extremely heavy and incredibly light: performative assemblies in dynamic environments," in *18th International Conference on Computer-Aided Architectural Design Research in Asia: Open Systems, CAADRIA 2013; Singapore; Singapore; 15 May 2013 through 18 May 2013*. Hong Kong: The Association for Computer-Aided Architectural Design Research in Asia (CAADRIA), 2013, pp. 469–478.

[39] F. Fleury, "Evaluation of the perpendicular flat vault inventor's intuitions through. large scale instrumented testing," in *Proceedings of the Third International Congress on Construction History*. Chicago, IL: Construction History Society of America, 2009, pp. 561–568.

[40] P. Song, C.-W. Fu, P. Goswami, J. Zheng, N. J. Mitra, and D. Cohen-Or, "Reciprocal frame structures made easy," *ACM Transactions on Graphics (TOG)*, vol. 32, no. 4, p. 94, 2013.

[41] R. Roelofs, "Three-dimensional and dynamic constructions based on leonardo grids," *International Journal of Space Structures*, vol. 22, no. 3, pp. 191–200, 2007.

[42] B. N. Delaunay and N. N. Sandakova, "Theory of stereohedra," *Trudy Matematicheskogo Instituta imeni VA Steklova*, vol. 64, pp. 28–51, 1961.

[43] M. W. Schmitt, "On space groups and dirichlet–voronoi stereohedra," Ph.D. dissertation, Berlin: Freien Universität Berlin, 2016.

[44] S. Adriaenssens, P. Block, D. Veenendaal, and C. Williams, *Shell structures for architecture: form finding and optimization*. Abingdon, United Kingdom: Routledge, 2014.

[45] B. Grünbaum and G. C. Shephard, *Tilings and patterns*. Austin, TX: W. H. Freeman and Company, 1987.

[46] R. Penne, "Configurations of few lines in 3-space. isotopy, chirality and planar layouts," *Geometriae Dedicata*, vol. 45, no. 1, pp. 49–82, 1993.

[47] E. Akleman, J. Chen, and J. L. Gross, "Block meshes: Topologically robust shape modeling with graphs embedded on 3-manifolds," *Computers & Graphics*, vol. 46, pp. 306–326, 2015.

[48] M. Conder and P. Dobcsányi, "Determination of all regular maps of small genus," *Journal of Combinatorial Theory, Series B*, vol. 81, no. 2, pp. 224–242, 2001.

[49] J. Richter-Gebert, "Combinatorial obstructions to the lifting of weaving diagrams," *Discrete & Computational Geometry*, vol. 10, no. 3, pp. 287–312, 1993.

[50] G. M. Ziegler, "Oriented matroids," *The Electronic Journal of Combinatorics*, pp. DS4–Sep, 2012.

Vinayak Krishnamurthy is an Assistant Professor in the J. Mike Walker '66 Department of Mechanical Engineering since 2016 and Computer Science and Engineering by Affiliation at Texas A&M University. He earned his Ph.D. in Mechanical Engineering in 2015 from Purdue University at West Lafayette, Indiana, USA. His research is at the intersection of geometric & topological modeling, human-computer interaction, and product & engineering design.

Ergun Akleman is a Professor in the Departments of Visualization & Computer Science and Engineering since 1995. He received my Ph.D. in Electrical and Computer Engineering from the Georgia Institute of Technology in 1992. His research is in the areas of shape modeling, image synthesis, artistic depiction, image based lighting, texture and tiles, computer aided caricature, and computer-aided architecture.

Sai Ganesh Subramanian is a graduate student in the J. Mike Walker '66 Department of Mechanical Engineering at Texas A&M University since 2018. He earned his Bachelors in Mechanical Engineering from the National Institute of Technology, Tiruchirappalli, India in May 2018. His area of research is geometric modeling, analysis, and additive manufacturing for generative design.

Matthew Ebert is currently an undergraduate student pursuing Bachelor of Science in the J. Mike Walker '66 Department of Mechanical Engineering at Texas A&M University. He is a 3D printing enthusiast with research interests in the fields of computer-aided design, additive manufacturing, and applied mechanics.

Jiaqi Cui is currently a graduate student pursuing Master of Science in the Department of Visualization at Texas A&M University. Her area of interest is visualization and rendering for architectural design.

Chia-an Fu is currently a graduate student pursuing Master of Science in the Department of Visualization at Texas A&M University. Her area of interest is the application of geometric modeling for architectural design.

Courtney Starrett is Associate Professor in the Department of Visualization at Texas A&M University and co-owner of Plural Studios. She has previously been on faculty at Seton Hall University and Winthrop University, SUNY New Paltz, Kendall College of Art and Design. She is an expert in additive manufacturing, aluminium & wax casting, and fabrication of silicone-based flexible parts.

APPENDIX

The principal Stress for each of the curved domain cases studied in Figure 18. Each figure has the three weaving patterns plain, twill, and satin. The monolithic case is also shown for each domain. The maximum, medium and maximum stresses were used since some of the cases are oriented in such a way that the force was applied in the Z direction while other cases Y was the direction of force. Using the maximum, medium, and minimum allow for greater comparison through all of the weaves and domains regardless of initial orientation.

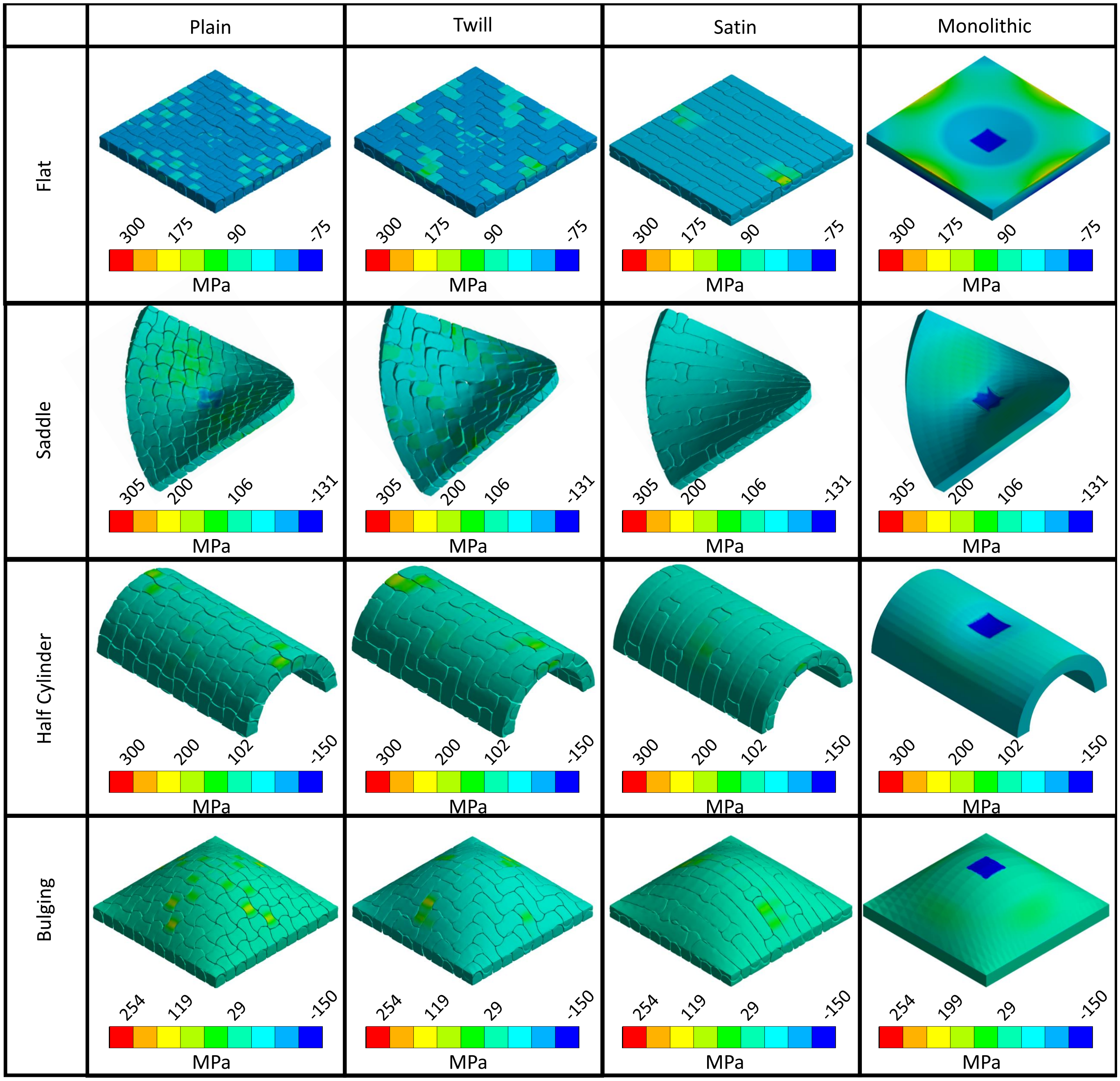

Fig. 20: The maximum principal stress for WovenTiles in comparison to monolithic blocks.

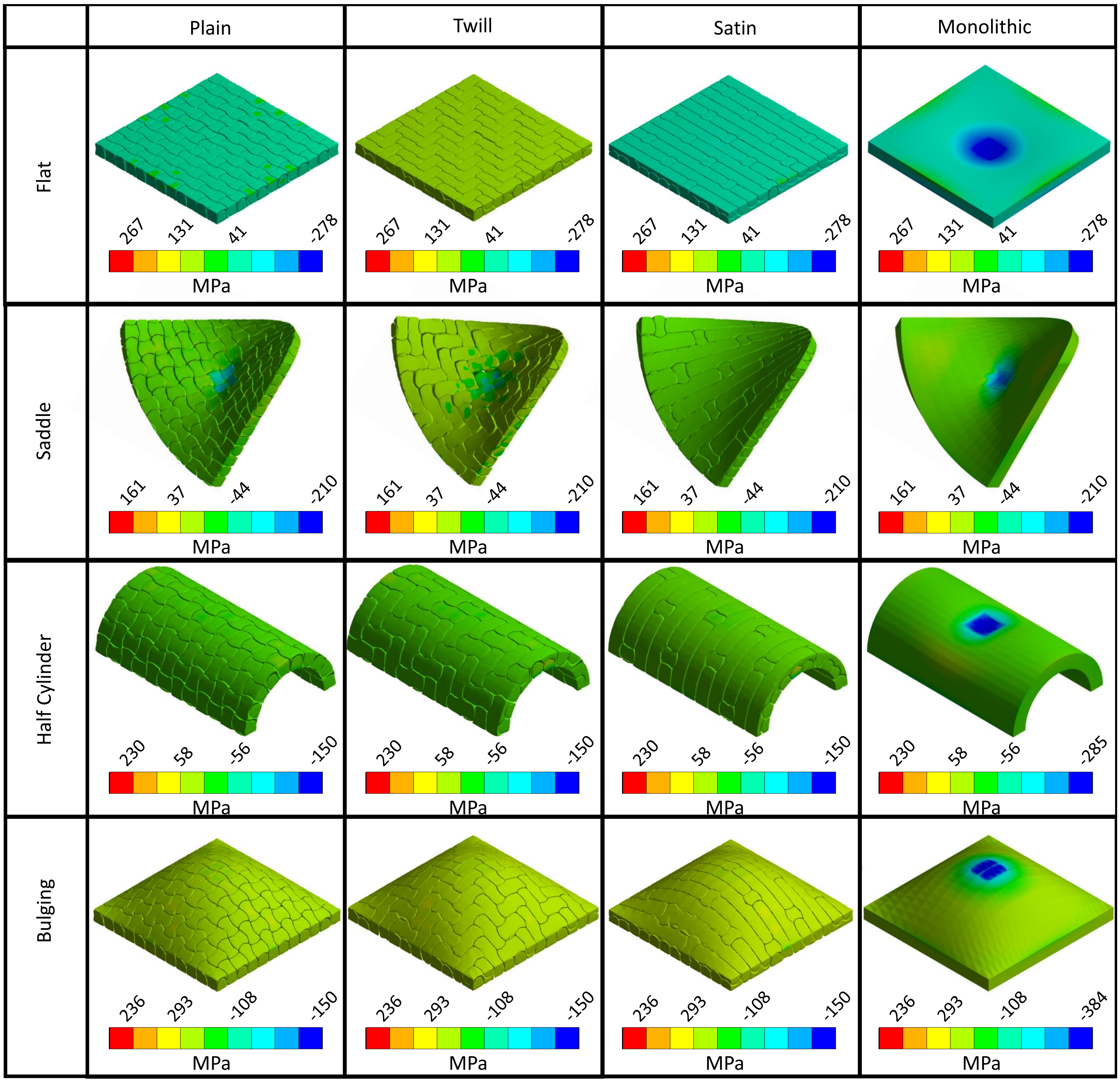

Fig. 21: The second-largest principal stress for WovenTiles in comparison to monolithic blocks.

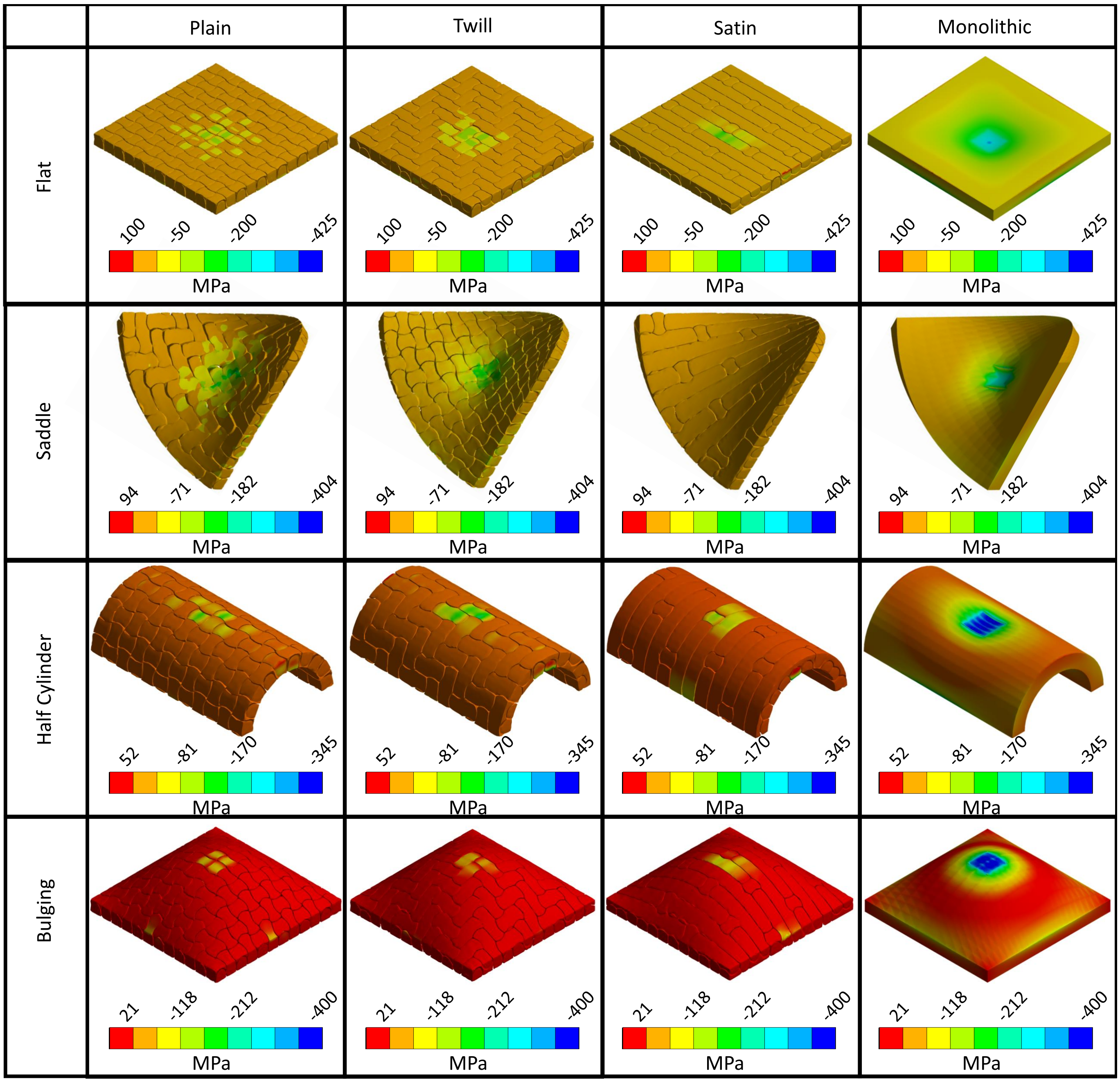

Fig. 22: The minimum principal stress for WovenTiles in comparison to monolithic blocks.